Chemical Science

ROYAL SOCIETY OF CHEMISTRY

EDGE ARTICLE

View Article Online
View Journal | View Issue

Cite this: *Chem. Sci.*, 2021, **12**, 11585

All publication charges for this article have been paid for by the Royal Society of Chemistry

Received 22nd June 2021
Accepted 20th July 2021

DOI: 10.1039/d1sc03394h

rsc.li/chemical-science

Molecular crystalline capsules that release their contents by light†

Akira Nagai,[a] Ryo Nishimura,[a] Yohei Hattori,[a] Eri Hatano,[a] Ayako Fujimoto,[a] Masakazu Morimoto,[b] Nobuhiro Yasuda,[c] Kenji Kamada,[d] Hikaru Sotome,[e] Hiroshi Miyasaka,[e] Satoshi Yokojima,[f] Shinichiro Nakamura[g] and Kingo Uchida *[a]

Here, we present single crystalline capsules of a photoresponsive molecule produced by simple recrystallization from organic solutions without direct human processing. During the crystal growth process, a movie was taken of the capsule taking in the organic solution. The capsules responded rapidly (<1 s) to the UV light stimuli and released the captured solution or solute. In principle, they can take in any substance dissolved in organic solvents, and their size can be controlled. Moreover, the capsule can be broken by multi-photon excitation using a near-infrared laser within the biological window. Furthermore, because the molecular packing in the crystal is unidirectional, the response can be controlled by the polarization of the light. This study shows the new potential of photoresponsive molecules.

Introduction

Photoresponsive molecules have been considered for a variety of applications, from memories[1] and switches[2] to molecular machines[3,4] and artificial intelligence.[5] In particular, assemblies of photoresponsive molecules can convert the photoreaction at the molecular level into the macroscopic dynamic behaviour of materials.[6,7] Among them, single crystals of photoresponsive molecules are the simplest form, and they can directly translate molecular structural changes into forces.[8–11] The most violent moves of crystals by light, including leaps and destruction, were named the photosalient effect by Naumov and co-workers.[12,13] However, it has been difficult to apply photosalient phenomena to a functional device. We have previously created a photosalient crystal with a cavity formed during the sublimation process and demonstrated the scattering of 1 μm-sized beads from inside the cavity by UV-irradiation.[14] This was a biomimetic system mimicking the seeds of *Impatiens*, except that the closed edge of the crystal was cut and the 'seeds' were artificially implanted by a capillary phenomenon by dipping the edge of the hollow crystal. In addition, there was no lid for the cavity, and thus it was always open.

Here, we have discovered a photosalient crystal that naturally takes in organic solutions during the recrystallization process. The capsule is sealed and can take in any solute in the solvent in principle. Such organic molecular crystals with sealed hollows have been known since the turn of the century,[15,16] but only recently have attempts been made to deliberately create and control them.[17,18]

The capsule released its contents in 1 second by UV irradiation. To show the potential of a bioengineering application, we demonstrate multiphoton response to near-infrared (NIR) light within a biological optical window, which is applied in photodynamic therapy.[19,20] To show the features of photoreactive single molecular crystals, reactivity control by linearly polarized light has also been demonstrated.

Although this research represents a basic scientific discovery, packing, moving, and releasing materials without touching them is a fundamental demand of technology. Photoresponsive molecular capsules have the potential to be used in a variety of applications that require the release of chemicals, such as soft robot parts,[21,22] drug delivery systems,[23,24] artificial

[a]*Department of Materials Chemistry, Faculty of Science and Technology, Ryukoku University, Seta, Otsu, Shiga 520-2194, Japan. E-mail: uchida@rins.ryukoku.ac.jp*
[b]*Department of Chemistry and Research Center for Smart Molecules, Rikkyo University, 3-34-1 Nishi-Ikebukuro, Toshima-ku, Tokyo 171-8501, Japan*
[c]*Japan Synchrotron Radiation Research Institute, 1-1-1 Kouto, Sayo-cho, Sayo-gun, Hyogo 679-5198, Japan*
[d]*Nanomaterials Research Institute (NMRI), National Institute of Advanced Industrial Science and Technology (AIST), Ikeda, Osaka 563-8577, Japan*
[e]*Graduate School of Engineering Science, Osaka University, Toyonaka, Osaka 560-8531, Japan*
[f]*School of Pharmacy, Tokyo University of Pharmacy and Life Sciences, 1432-1 Horinouchi, Hachioji, Tokyo 192-0392, Japan*
[g]*Nakamura Laboratory, RIKEN Cluster for Science, Technology and Innovation Hub, 2-1 Hirosawa, Wako, Saitama 351-0198, Japan*

† Electronic supplementary information (ESI) available. CCDC 1983516, 1983522–1983525, 1983529, 1983556, 1983598, 2040177 and 2040178. For ESI and crystallographic data in CIF or other electronic format see DOI: 10.1039/d1sc03394h

nerves,[25,26] artificial muscles,[27,28] and human–machine interfaces that convey taste and smell.[29,30]

Results and discussion

Characterization of crystalline capsules

We prepared a new diarylethene with *m*-trimethylsilylphenyl groups at both ends of the molecule (**1o**) (Fig. 1a). Diarylethenes are extensively studied compounds with photochromism, which show a reversible transformation between open and closed forms by photoirradiation.[1] The diarylethene **1o** showed photochromism between **1o** and **1c** in solid and in solution (Fig. 1a and S1†). When the crystals were continuously irradiated with a UV lamp ($\lambda = 313$ nm), they turned blue and then showed slight bending followed by fragmentation (a photosalient effect).

When we tried to obtain single crystals of **1o** using a common evaporation method from various organic solvents such as hexane, ethyl acetate and dichloromethane at room temperature, we found a certain portion of them had capsule structures. From a hexane solution, 7.7% of the crystals (668 out of 7967) had capsule structures (see also Experimental section). Single-crystal X-ray diffraction (XRD) analysis showed that crystalline capsules prepared from these solvents have the same crystal structure as non-capsule crystals (Table S1†).

To ascertain that the capsule had a closed structure without holes, we cracked a crystal (Fig. 1b) with a needle, consequently, air bubbles entered the hollow as the liquid inside (hexane solution) began to flow out (Fig. 1c, ESI Movie S1†). A cross-section scanning electron microscopy (SEM) image of the crystal shows a hollow structure (Fig. 1d and S2a–f†).

We observed the formation process of the capsule structure by optical microscopy and captured the moment of formation of the primary liquid inclusions[31] (Fig. 1e, ESI Movie S2†). The hollows were formed parallel to the fast-growing axis similarly to the recent reports of inclusions in organic molecular crystals,[16,18] and the formation mechanism of the crystalline capsules was in accordance with these references where the formation mechanism is attributed to the inhomogeneous growth of crystals. In this work as well, the appearance of cavities due to inhomogeneous growth of the crystals, and trapping of the solution in the cavities were observed.

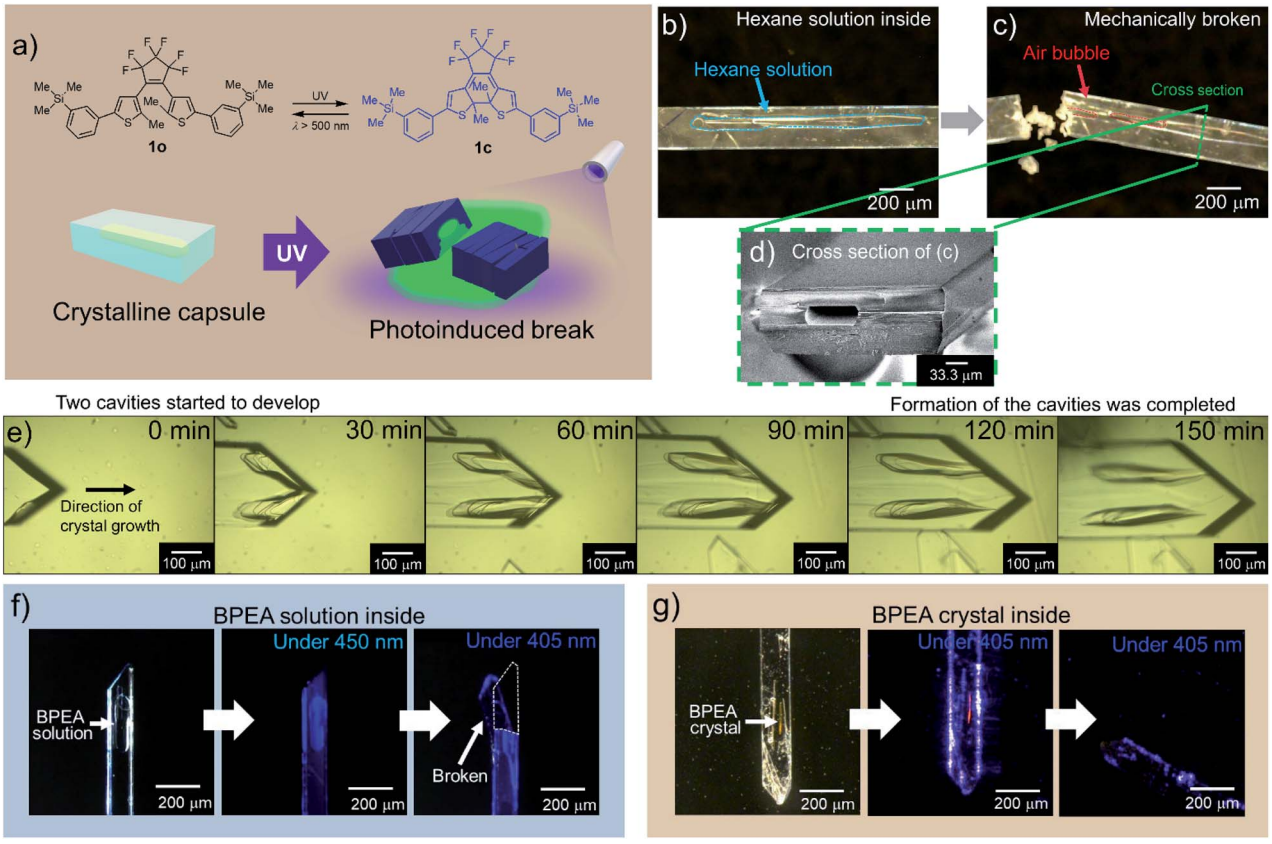

Fig. 1 The formation and response of crystalline capsules of diarylethene **1**. (a) Molecular structures of open-(**1o**) and closed-ring isomer (**1c**) and photo-release from a crystalline capsule. (b) A crystalline capsule of **1o** including hexane solution of **1o**. (c) After the capsule was broken with a needle, hexane solution leaked, and the intrusion of air bubbles into the capsule was observed (ESI Movie S1†). (d) Cross-section SEM image of a crystalline capsule shown in (c); hole size was *ca.* 30 × 70 μm. (e) Observation of the formation of crystalline capsule. A crystal was grown along with the formation of two capsule cavities (ESI Movie S2†). (f) A **1o** crystal encapsulating **BPEA** in solution (left). Crystal irradiated with 450 nm light (centre). Crystal irradiated with 405 nm LED light, which released solution by a photosalient phenomenon (right). See also ESI Movie S3.† (g) A crystalline capsule of **1o** encapsulating a **BPEA** crystal (left). Crystal irradiated with 405 nm light (centre). Continued irradiation with the 405 nm light, where the crystal released the contained crystal of **BPEA** by a photosalient phenomenon (right). See also ESI Movie S4.†

Crystalline capsules containing fluorescent dyes

We prepared crystalline capsules containing 9,10-bis(phenylethynyl)anthracene (**BPEA**), a highly fluorescent hydrophobic dye, by adding **BPEA** in hexane, a recrystallization solvent. These crystals had the same crystal structure as the previous crystals (Table S2†). The wavelength of the absorption edge of **BPEA** is longer than that of **1o**, and the absorption tail of **BPEA** exceeds 450 nm where **1o** has no absorption. The emission wavelength of **BPEA** is also longer than that of **1o** (Fig. S1c and S2j†). Therefore, when the crystalline capsule was irradiated with 450 nm LED light, blue fluorescence from **BPEA** in the hexane inside the capsule was observed (Fig. 1f). When 405 nm LED light was applied to activate the capsule body of **1o**, it released an encapsulated hexane solution of **BPEA** showing a photosalient phenomenon (ESI Movie S3†). In the event, capsules always cracked perpendicular to the long axis of the capsules.

Surprisingly, we found some crystals of **1o** encapsulating orange **BPEA** crystals (Fig. 1g and S2g–i†) in the same recrystallization solution as the crystals encapsulating **BPEA** in solution. By irradiation of 405 nm LED light to the capsules, orange fluorescence from the **BPEA** crystals in the capsule was observed, followed by scattering from the crystalline capsule of **1o** to release the **BPEA** crystals showing photosalient phenomena (ESI Movie S4†).

To visually demonstrate the photo-induced property of a crystalline capsule of **1o**, we made crystalline capsules containing 5(6)-carboxyfluorescein (**5(6)-FAM**), a fluorescent dye used as a fluorescent tracer. The crystalline capsules were prepared from an acetone–methanol (3 : 1) solution of **1o** and **5(6)-FAM** in 21% yield. If a chemical can be dissolved in a solvent and coexist with **1o** under recrystallization conditions, it is assumed that the capsule can take up any such chemical in solution. A crystal was floated on an aqueous buffer droplet (pH = 9.18 at 25 °C) under a microscope, and the green fluorescence of **5(6)-FAM** was visualized by 450 nm LED light, which does not induce the photoreaction of **1o** (Fig. 2a). Upon UV irradiation, the green fluorescence emission from **5(6)-FAM** was diffused in the aqueous buffer that appeared after the capsule was broken. The fluorescence of **5(6)-FAM** expanded on the water surface around the crystal, indicating successfully photoinduced release from the crystalline capsule (Fig. 2b, ESI Movie S5†). These crystalline capsules can scatter fluorescent beads (1 μm-diameter) similarly to the previous cup-shaped crystals[14] by hand processing (Fig. S3a, ESI Movie S6†), which visually demonstrates that the crystals can release both liquid and solid matters.

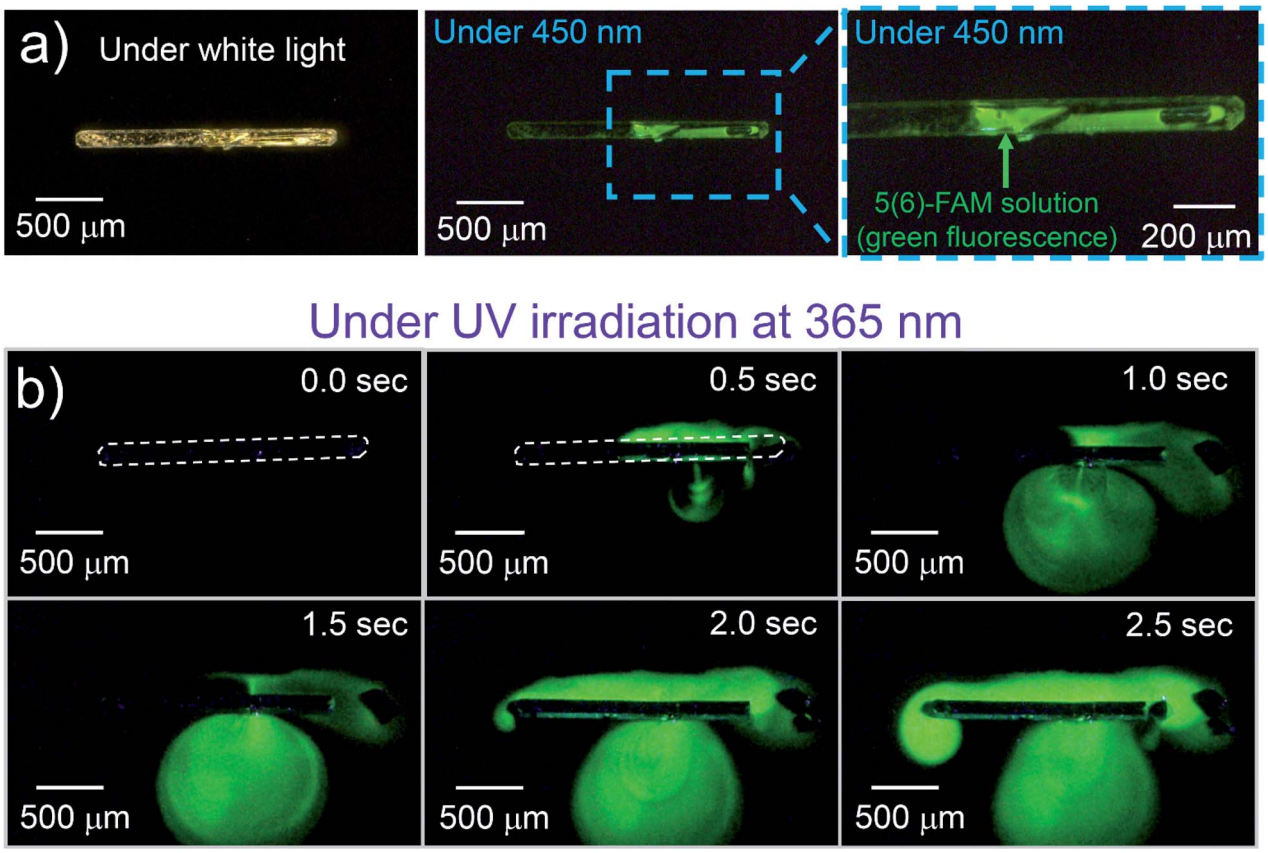

Fig. 2 A crystalline capsule of **1o** encapsulating fluorescent dye solution. (a) A **1o** crystal encapsulating **5(6)-FAM** solution and the crystal irradiated with 450 nm light, which does not induce the photoreaction of **1o**. Green fluorescence was observed from **5(6)-FAM** solution. (b) Crystal irradiated with 365 nm light, which induces the photoreaction of **1o** to release the solution by a photosalient phenomenon. The fluorescence area from **5(6)-FAM** expanded on the water surface over time (ESI Movie S5†).

To control the crystal size, we changed a recrystallization period to obtain crystalline capsules. When the crystalline capsules containing **5(6)-FAM** were prepared by recrystallization from the mixture of acetone and methanol dissolving the dye, the sizes of the obtained capsules were 2 mm in length and 300–400 μm in width for a 48 h recrystallization period. The sizes of the capsules were successfully reduced to less than 400 μm in length and less than 50 μm in width by shortening the recrystallization period to 12 h and filtering the solutions after this period. Elongation of the period induced an incremental increase in the maximum size of the crystals, with smaller crystals coexisting with them. The smaller capsules also released the **5(6)-FAM** they contained, which was clearly observed by the expansion of the cloud-like green fluorescent zone around the crystal upon UV irradiation (Fig. S3b, ESI Movie S7†).

Multi-photon excitation

We used a femtosecond laser pulse at 802 nm instead of UV light to break the crystalline capsules by multiphoton absorption. When the capsule of **1o** was irradiated with a laser (Fig. 3a), the capsule turned blue and was broken, showing a photosalient phenomenon (Fig. 3b, ESI Movie S8†). During laser irradiation, the rise in the capsule's temperature was only 1.6 °C as monitored by thermography (Fig. S4a and b†). Therefore, the laser excites the molecules efficiently by multiphoton absorption and only slightly heats the crystal. No phase transition accompanied by laser irradiation, which was consistent with the DSC measurement showing no peak around this temperature region (23.9–25.5 °C; Fig. S4c†).

From the two-photon absorption (TPA) cross section of **1o** separately measured in dichloromethane solution, the ratio of the number of excited **1o** molecules to that of the molecules in the ground state before irradiation by a single laser pulse was estimated to be 2.36×10^{-6} (see ESI and Fig. S4d†). With this value, 12% of **1o** molecules could be excited by the NIR laser in 50 s, which was the time it took for the crystal to show a photosalient effect (corresponding to 50 000 pulses). This value is sufficient for the crystal to exhibit the photosalient phenomenon described later. The response to NIR light within the biological window (650–1350 nm),[20,32] which penetrates biological tissue, is an important factor for applications operating in living bodies such as a drug delivery system. The NIR multiphoton excitation can be used to induce photo-release from the crystalline capsules.

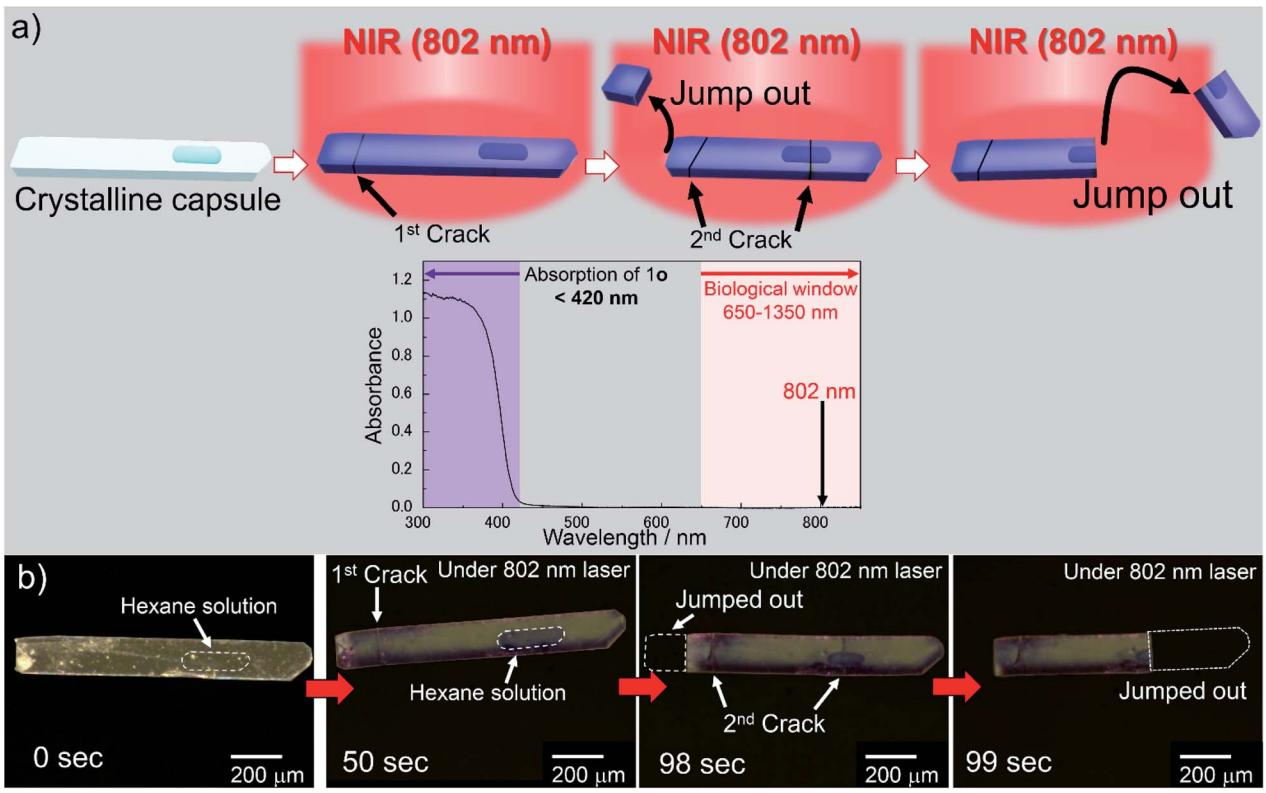

Fig. 3 Photoresponse of a crystalline capsule upon NIR light. (a) Photosalient phenomenon of a crystalline capsule of **1o** by multiphoton absorption using femtosecond NIR laser (802 nm) and absorption spectrum of **1o** in crystalline state. Absorption wavelength of **1o** (<420 nm) is shown in purple and the biological window (650–1350 nm) is shown in pink in the spectrum. Crystal of **1o** was excited by multiphoton absorption with femtosecond NIR (802 nm) laser. Two photons of 802 nm correspond to the one photon of 401 nm, which is the tail of the absorbance of the capsule. (b) A crystalline capsule of **1o** used in this experiment (left). Upon irradiation of the femtosecond NIR laser (802 nm), the crystalline capsule of **1o** was coloured blue (centre part of dark domain is the cavity including hexane solution of **1o**). The initial crack was observed at 50 s, and the left side jumped out immediately. The second cracks were observed at 98 s. Then, the missing part of the crystal showed a photosalient phenomenon (99 s). See also ESI Movie S8.†

X-ray crystallography

To clarify the mechanism of photoresponse in the crystal **1o**, we performed XRD measurements on a single crystal of **1o** before and after irradiation of UV light ($\lambda = 400$ nm) for 10 s and 20 s (orthorhombic, space group *Pbcn*, $Z = 8$, Table S3†). Upon further UV irradiation, the crystal broke. The conversion rate to **1c** after the 20 s irradiation (*ca.* 10%; Table S3†) was consistent with the conversion rate by the femtosecond NIR laser (*ca.* 12%), showing a photosalient effect. Then, the *a*-axis and *b*-axis of the unit cell expanded by 0.77% and 0.81%, respectively, while the *c*-axis contracted by 1.30%, and cell volume expanded by 0.26% (Table S3†). These changes were much larger than those of the photosalient crystal we previously reported.[14] The scattering speed of **1o** was 1.0 m s^{-1}, which is similar to the previous results.

Face-indexing of a single crystal revealed that the widest surface of the crystal was (001) face, and the thickness direction of the crystal was determined to be the *c*-axis. The longer and

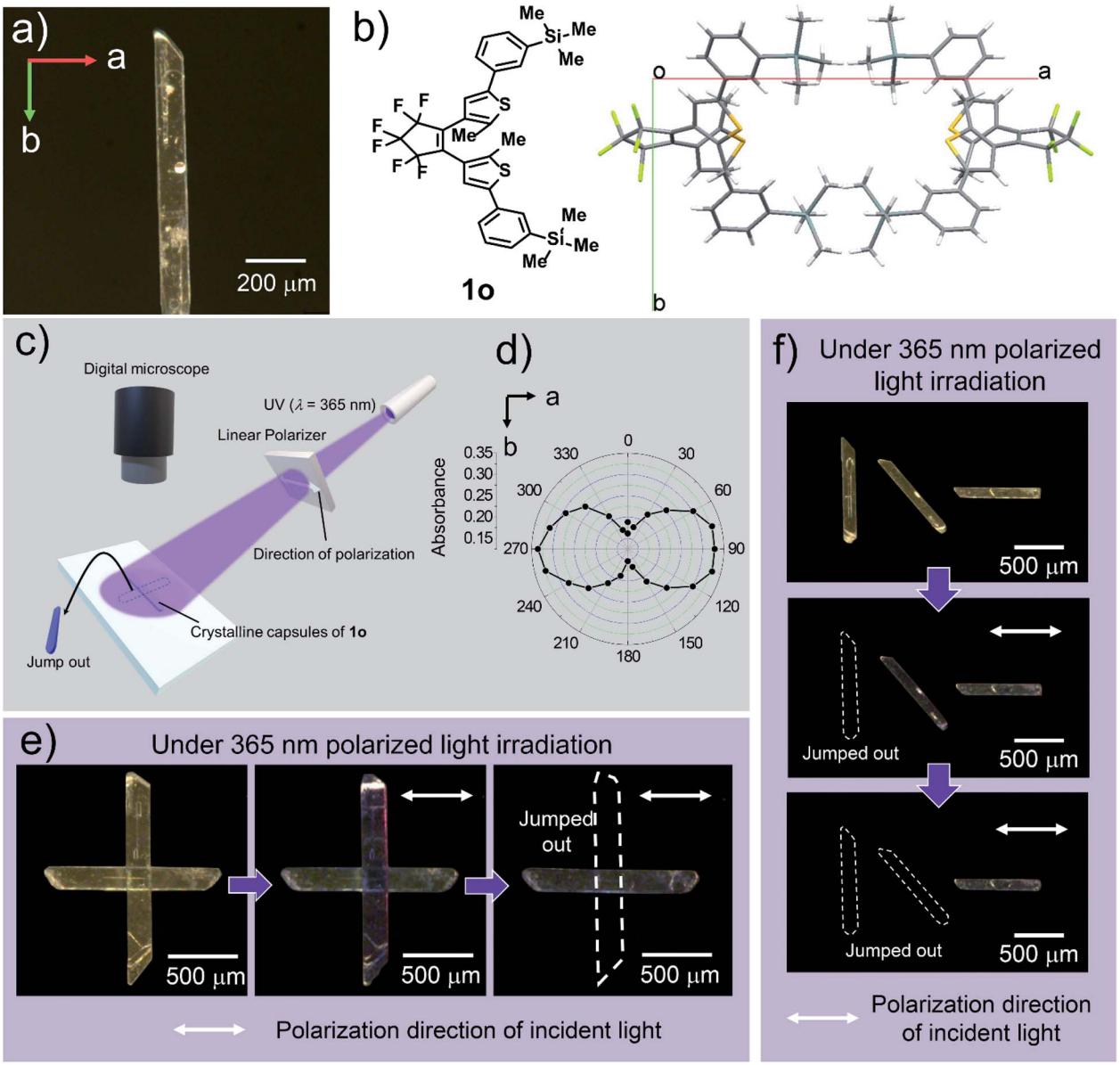

Fig. 4 Photoresponse of a crystalline capsule upon polarized light. (a) Relationship between long and short axes of the crystalline capsule and *a*- and *b*-axes of the crystal lattice. (b) Molecular packing of **1o** in the crystal viewed from the (001) surface. (c) Schematic diagram of observed photosalient effect depending on polarization direction of UV light. Polarization direction is parallel to the white double arrow. (d) Polar plot of action spectrum of the crystal of **1o**. The colouring of the crystal is dependent on the direction of polarized UV light. (e) Two crystalline capsules of **1o** were placed orthogonally to each other on a slide glass. When 365 nm linearly polarized light was irradiated, the crystal which has its long axis perpendicular to the polarization direction showed colouration followed by jumping away (ESI Movie S9†). (f) Three crystalline capsules were placed together and oriented at angles 45° apart. The crystal whose long axis was perpendicular to the polarization direction jumped away at first, followed by the one rotated 45° from the polarization direction. The crystal whose long axis was parallel to the polarization direction remained largely unchanged (ESI Movie S10†).

shorter axes of the widest surface of the crystal were found to be the *b*-axis and *a*-axis of the unit cell, respectively (Fig. 4a). Since the long axis of the crystal along the *b*-axis expanded, it was observed that the crystals bent in the direction opposite to the light source when the wide (001) surface was irradiated with UV light (Fig. S5†). It is assumed that the crystal breaks when the structure can no longer withstand the accumulated strain. The cracks were generated perpendicular to the long axis of the crystalline capsules, which is along the *b*-axis.

Control by linear polarization of light

The photoresponse of the crystal of **1o** depends on the polarization direction of light, since all of the molecules are regularly aligned in the single crystals (Fig. 4b). When linearly polarized 365 nm light was irradiated on the (001) surface of the photo-irradiated crystal, the **1o** molecule reacted strongly to this light when polarized parallel to the *a*-axis (Fig. 4c) as shown in the polar plot of action spectrum (Fig. 4d).

To demonstrate the controllability of the photosalient phenomena of the crystalline capsules by the polarization direction of the light, we irradiated crystalline capsules placed on a slide glass with linearly polarized 365 nm UV light and then observed the photosalient effect (jumping) through a microscope (Fig. 4c). When two crystalline capsules were positioned orthogonally to each other (Fig. 4e), the crystal whose long axis (*b*-axis) was perpendicular to the polarization direction showed colouration followed by jumping out from the view, whereas the other crystal showed almost no change (Fig. 4d, ESI Movie S9†).

Similarly, when three crystalline capsules were placed together and oriented at angles 45° apart, the crystal whose long axis (*b*-axis) was perpendicular to the polarization direction initially showed the photosalient phenomenon of jumping out of the screen, and then the crystal placed at the oblique angle showed this photosalient effect. The crystal placed parallel to the polarization direction only showed observable cracking on the surface (Fig. 4f, ESI Movie S10†). These results demonstrate that the photosalient phenomena of the crystalline capsules can be controlled by the polarization direction of the light.

Dependence on polarization direction of the light could also be observed through the bending behaviour of the crystals. Some crystalline capsules of **1o** were placed on the tips of glass capillaries, and the wide (001) surface was irradiated with 365 nm UV light through a linear polarizer. When the polarization direction was parallel to the *a*-axis, the crystal bent and then broke (Fig. S6a–c†). On the other hand, when the polarization direction was perpendicular to the *a*-axis, the crystal was slightly bent but not broken (Fig. S6d and e†). The crystal did not break even after irradiation for 40 s, but when the polarizer was rotated 90° (to make it parallel to the *a*-axis), it bent further and then broke showing photosalient phenomenon (Fig. S6f and g†).

Conclusions

In summary, we prepared a novel diarylethene **1o**, found that it forms liquid inclusions, and succeeded in encapsulating chemicals dissolved in or precipitated from recrystallization solvents. The sizes of these "crystalline capsules" were controllable by the recrystallization period. We also demonstrated the release of chemicals due to a photosalient effect by irradiation with UV light and by multiphoton absorption with an NIR laser. The photoresponse was selective to the linear polarization of incident light. Compared to previously reported photo-release systems, crystalline capsules have novel characteristics: the ability in a solid wall to completely separate internal and external spaces, the capability to contain a variety of chemicals soluble in organic solvents, rapid release of chemicals within 1 second, and crystal-orientation-dependent reactivity to linearly polarized light. We expect these crystalline capsules to be of great use in the future in various scientific fields such as materials engineering, medicine, and robotics.

Experimental

Synthesis of 1,2-bis(2-methyl-5-(phenyl-3-trimethylsilyl)thien-3-yl)perfluorocyclopentene (1o)

In an argon gas atmosphere, 1.50 g (3.43 mmol, 1.0 eq.) of 1,2-bis(5-chloro-2-methylthien-3-yl)perfluorocyclopentene (**2o**), prepared according to a previous paper,[33] was dissolved in 50 mL of anhydrous diethyl ether in a 100 mL three-necked flask. The solution was cooled in an ice-salt bath to around −6 °C. To the solution, 6.43 mL (10.3 mmol, 3.0 eq.) of 1.6 M *n*-BuLi hexane solution was gradually added over 15 min, followed by stirring for 1 h at the above temperature. To the solution, 2.76 mL (10.3 mmol, 3.0 eq.) of $B(OBu)_3$ was gradually added over 5 min followed by stirring, and the mixture was allowed to warm to room temperature. After stirring at room temperature for an additional 1 h, 10 mL of water was added. Then the solvents in the three-necked flask were removed *in vacuo*. The flask was placed under an argon gas atmosphere, then 1.81 g (7.89 mmol, 2.3 eq.) of 1-bromo-3-(trimethylsilyl)benzene (**3**), prepared according to a previous paper,[34] 40 mL of 20 wt% Na_2CO_3 aq. solution, 40 mL of THF, and 0.28 g (0.24 mmol, 0.07 eq.) of tetrakis(triphenylphosphine)palladium (0) were added successively. Then the mixture solution was refluxed (70 °C) for 18 h. Next, the mixture was allowed to cool to room temperature followed by removal of THF *in vacuo*. The mixture was extracted with diethyl ether (50 mL × 4), and the combined organic extracts were washed with 50 mL of saturated saline solution. The separated organic layer was dried over sodium sulfate anhydrous. After the sodium sulfate was removed by filtration, solvents were removed to obtain 4.47 g of a brownish solid mixture containing **1o**. After purification by silica gel chromatography (Wakogel® C-200 (75–150 μm), eluent: hexane, φ = 3.5 cm, h = 35 cm), 1.21 g of the crude **1o** was obtained as white powder in 53% yield. The crude **1o** was purified by recrystallization from hexane solution to obtain 717 mg of colourless needle-shaped crystals of **1o** in 31% yield.

mp: 179.0–180.1 °C; ^{1}H NMR (400 MHz, $CDCl_3$): δ 0.29 (s, 18H), 1.99 (s, 6H), 7.26 (s, 2H), 7.37 (t, J = 7.4 Hz, 2H), 7.45 (d, J = 7.4 Hz, 2H), 7.52 (m, 2H), 7.63 (s, 2H); ^{13}C NMR (100 MHz, $CDCl_3$): δ −1.05, 14.7, 122.5, 126.0, 126.3, 128.5, 130.5, 132.8, 133.1, 141.4, 141.8, 142.7; ^{19}F NMR (376 MHz, $CDCl_3$): δ −135.1

(s, 2F), −113.2 (s, 4F); found: C, 59.43; H 5.02. Calc. for $C_{33}H_{34}F_6S_2Si_2$: C, 59.61; H, 5.15%.

Photochromic property of 1 in solution

The newly prepared diarylethene **1o** showed photochromism in a hexane solution (Fig. S1c†). Absorption maximum wavelengths of **1o** and **1c** were 284 nm ($\varepsilon = 3.78 \times 10^4$ M^{-1} cm^{-1}) and 580 nm ($\varepsilon = 1.76 \times 10^4$ M^{-1} cm^{-1}), respectively. The quantum yields of cyclization and cycloreversion reactions were 0.65 and 7.9×10^{-3}, respectively. The intensities of the irradiation light were estimated by comparing the photochromic reactions of diarylethenes as actinometers.[35]

Preparation of crystals of 1o with capsule structures

The crystals were obtained by recrystallization from organic solvents such as hexane, ethyl acetate, and dichloromethane. For example, 100 mg of **1o** was dissolved in 8 mL of hexane, and solvents were allowed to be removed at room temperature under normal pressure to obtain 7967 crystals of **1o** after two days. The number of crystals on the optical microscopic images was counted. Among them, 668 crystals (7.7%) had capsule structures.

Crystalline capsules containing 9,10-bis(phenylethynyl) anthracene (BPEA)

Diarylethene **1o** 100 mg (1.88×10^{-2} M) and **BPEA** 0.05 mg (1×10^{-8} M) were dissolved in 8 mL of hexane, and recrystallization was carried out for two days to obtain 28 mg of crystals. They include the solution or crystal of **BPEA** in a capsule structure.

Crystalline capsules containing 5(6)-carboxyfluorescein (5(6)-FAM)

Diarylethene **1o** 100 mg (1.88×10^{-2} M) and **5(6)-FAM** 37.6 mg (1.25×10^{-2} M) were dissolved in a mixture of 6 mL of acetone and 2 mL of methanol, and recrystallization was carried out for two days to obtain 44 mg of crystals. They include the solution of **5(6)-FAM** in the capsule structure. A crystal capsule was floated on the surface of a basic borate pH standard buffer solution (pH = 9.18 at 25 °C), since fluorescein derivatives are known to increase fluorescence intensity under basic conditions, and then UV light (λ = 365 nm, 550 mW cm^{-2}) was irradiated (Fig. S2b†).

Author contributions

A. N. and K. U. designed the project. A. N. synthesized the compound **1o**, and prepared crystalline capsules with and without inclusions by recrystallization. A. N. also observed the photoresponse of the crystalline capsules. M. M. determined the crystalline structure of **1o** by X-ray analysis of non-capsuled crystals. N. Y., A. N., Y. H., R. N., A. F., K. U. performed the synchrotron radiation experiments at SPring-8. K. K., A. N., R. N. observed the two-photon cross section of **1o** in chloroform solution. A. N., R. N., H. S., H. M, performed multiphoton excitation experiment using a femtosecond laser system. A. N., Y. H., S. Y., S. N. and K. U. wrote the manuscript. All authors discussed the results and commented on the manuscript.

Conflicts of interest

There are no conflicts to declare.

Acknowledgements

This work was supported by Supported Program for the Strategic Research Foundation at Private Universities from Ministry of Education, Culture, Sports, Science and Technology, Japan (KU), JSPS KAKENHI Grant JP26107012 in Scientific Research on Innovative Areas "Photosynergetics" (KU), CREST program grant JPMJCR17N2 of the Japan Science and Technology Agency (KU), JSPS KAKENHI grant JP18J20078 in JSPS Research Fellow (RN), JSPS KAKENHI grant JP18H01943 (KK). The synchrotron radiation experiments were performed using the BL02B1, BL40B2, and BL40XU beamlines of SPring-8 with the approval of the Japan Synchrotron Radiation Research Institute (JASRI) (Proposal Nos. 2016A1080, 2016B1125, 2018A1104, 2018A1208, 2018B1091, 2018B1092, 2018B1674, 2019A1110, 2019A1670, and 2019A1741).

Notes and references

1 M. Irie, T. Fukaminato, K. Matsuda and S. Kobatake, *Chem. Rev.*, 2014, **114**, 12174–12277.
2 B. L. Feringa and W. R. Browne, *Molecular Switches*, WILEY-VCH Verlag & Co. KGaA, 2nd edn, 2011.
3 J. Chen, F. K.-C. Leung, M. C. A. Stuart, T. Kajitani, T. Fukushima, E. van der Giessen and B. L. Feringa, *Nat. Chem.*, 2018, **10**, 132–138.
4 F. Lancia, A. Ryabchun and N. Katsonis, *Nat. Rev. Chem.*, 2019, **3**, 536–551.
5 K. Uchiyama, H. Suzui, R. Nakagomi, H. Saigo, K. Uchida, M. Naruse and H. Hori, *Sci. Rep.*, 2020, **10**, 2710.
6 Y. Yu, M. Nakano and T. Ikeda, *Nature*, 2003, **425**, 145.
7 A. H. Gelebart, D. J. Mulder, M. Varga, A. Konya, G. Vantomme, E. W. Meijer, R. L. B. Selinger and D. J. Broer, *Nature*, 2017, **546**, 632–636.
8 S. Kobatake, S. Takami, H. Muto, T. Ishikawa and M. Irie, *Nature*, 2007, **446**, 778–781.
9 M. Morimoto and M. Irie, *J. Am. Chem. Soc.*, 2010, **132**, 14172–14178.
10 F. Terao, M. Morimoto and M. Irie, *Angew. Chem., Int. Ed.*, 2012, **51**, 901–904.
11 R. Nishimura, A. Fujimoto, N. Yasuda, M. Morimoto, T. Nagasaka, H. Sotome, S. Ito, H. Miyasaka, S. Yokojima, S. Nakamura, B. L. Feringa and K. Uchida, *Angew. Chem., Int. Ed.*, 2019, **58**, 13308–13312.
12 P. Naumov, S. C. Sahoo, B. A. Zakharov and E. V. Boldyreva, *Angew. Chem., Int. Ed.*, 2013, **52**, 9990–9995.
13 P. Naumov, S. Chizhik, M. K. Panda, N. K. Nath and E. Boldyreva, *Chem. Rev.*, 2015, **115**, 12440–12490.
14 E. Hatano, M. Morimoto, T. Imai, K. Hyodo, A. Fujimoto, R. Nishimura, A. Sekine, N. Yasuda, S. Yokojima,

S. Nakamura and K. Uchida, *Angew. Chem., Int. Ed.*, 2017, **56**, 12576–12580.
15 G. G. Z. Zhang and D. J. W. Grant, *Cryst. Growth Des.*, 2005, **5**, 319–324.
16 Y. Wang, N. Zhang, B. Hou, Q. Yin, J. Gong and W. Tang, *CrystEngComm*, 2020, **22**, 1991–2001.
17 F. Tong, W. Li, Z. Li, I. Islam, R. O. Al-Kaysi and C. J. Bardeen, *Angew. Chem., Int. Ed.*, 2020, **59**, 23035–23039.
18 J. Cooper, L. Bome and G. Coquerel, *Cryst. Growth Des.*, 2020, **20**, 7120–7128.
19 F. Heinemann, J. Karges and G. Gasser, *Acc. Chem. Res.*, 2017, **50**, 2727–2736.
20 J. Shi, X. Sun, S. Zheng, L. Song, F. Zhang, T. Madl, Y. Zhang, H. Zhang and M. Hong, *ACS Appl. Bio Mater.*, 2020, **3**, 5995–6004.
21 D. Rus and M. T. Tolley, *Nature*, 2015, **521**, 467–475.
22 L. Yu, P. Si, L. Bauman and B. Zhao, *Langmuir*, 2019, **36**, 3279–3291.
23 C. Englert, I. Nischang, C. Bader, P. Borchers, J. Alex, M. Pröhl, M. Hentschel, M. Hartlieb, A. Traeger, G. Pohnert, S. Schubert, M. Gottschaldt and U. S. Schubert, *Angew. Chem., Int. Ed.*, 2018, **57**, 2479–2482.
24 M. J. Mitchell, M. M. Billingsley, R. M. Haley, M. E. Wechsler, N. A. Peppas and R. Langer, *Nat. Rev. Drug Discovery*, 2021, **20**, 101–124.
25 Y. Lee and T.-W. Lee, *Acc. Chem. Res.*, 2019, **52**, 964–974.
26 M. Dong, B. Shi, D. Liu, J.-H. Liu, D. Zhao, Z.-H. Yu, X.-Q. Shen, J.-M. Gan, B.-l. Shi, Y. Qiu, C.-C. Wang, Z.-Z. Zhu and Q.-D. Shen, *ACS Nano*, 2020, **14**, 16565–16575.
27 D. Kaneko, J. P. Gong and Y. Osada, *J. Mater. Chem.*, 2002, **12**, 2169–2177.
28 L. Hines, K. Petersen, G. Z. Lum and M. Sitti, *Adv. Mater.*, 2017, **29**, 1603483.
29 C. T. Vi, D. Ablart, E. Gatti, C. Velasco and M. Obrist, *Int. J. Hum. Comput. Stud.*, 2017, **108**, 1–14.
30 L. Guerrini, E. Garcia-Rico, N. Pazos-Perez and R. A. Alvarez-Puebla, *ACS Nano*, 2017, **11**, 5217–5222.
31 V. B. Sisson, R. W. Lovelace, W. B. Maze and S. C. Bergman, *Geology*, 1993, **21**, 751–754.
32 J.-C. Boyer, M.-P. Manseau, J. I. Murray and F. C. J. M. van Veggel, *Langmuir*, 2010, **26**, 1157–1164.
33 L. N. Lucas, J. van Esch, R. M. Kellogg and B. L. Feringa, *Tetrahedron Lett.*, 1999, **40**, 1775–1778.
34 P. A. A. Klusener, J. C. Hanekamp, L. Brandsma and P. v. R. Schleyer, *J. Org. Chem.*, 1990, **55**, 1311–1321.
35 T. Sumi, Y. Takagi, A. Yagi, M. Morimoto and M. Irie, *Chem. Commun.*, 2014, **50**, 3928–3930.